10% FBS at a concentration of 16,000 cells/cm^2 and incubated for 4 hr. The medium then was replaced with 70% DMEM supplemented with 10% FBS containing $CaCl_2$ at concentrations of 1.8 mM and 3.6 mM. The cells were exposed to 100 μg/mL ZnO NPs just after the medium replacement. After 24 hr, the cells were washed with phosphate-buffered saline (PBS) twice and then treated with DMEM containing 500 nM of the CellRox Deep Red reagent (Life Technologies, Carlsbad, CA, USA) for intracellular ROS staining. After 25 min, PI (a final concentration of 2 μg/mL) was added to stain the dead cells. The cells were collected and washed with PBS buffer twice, and then fluorescence intensity was measured by fluorescence-activated cell sorting (FACS).

DNA microarray analysis

The DNA microarray procedure has been described in detail previously (Hanagata *et al.*, 2011). Briefly, total RNA was extracted with ISOGEN (Nippon Gene, Tokyo, Japan). The RNA was amplified with the Animo Allyl MessageAmp II aRNA amplification kit (Thermo Fisher Scientific, Waltham, MA, USA) and then labeled with Cy3 and Cy5. Whole genome-scale gene expression analysis was performed with the Whole Human Genome Microarray Kit 4x44K (Agilent, Santa Clara, CA, USA). The fluorescent intensity of Cy3 and Cy5 was scanned using GenePix 4000B (Molecular Devices, Sunnyvale, CA, USA) at 10-μm resolution at three levels. The spots in the scanned image were detected using GenePix Pro (Molecular Devices). Expression data were globally normalized, and a locally weighted scatterplot smoothing (LOWESS) adjustment was applied. The DNA microarray experiment was carried out twice. Only genes whose expression level ratios from the two trials were less than double were identified as reproducible genes. The expression level ratios of these genes were set as the average value for the two trials. Genes whose expression level was 2X or 0.5X were extracted as upregulated or downregulated genes. Genes with altered expression were placed into GO biological process categories using the PANTHER gene expression analysis/compare gene lists.

RESULTS

Effect of the dispersion medium used for ZnO NPs on the toxicity of the NPs

ZnO NPs were dispersed in five different media: H_2O, 10% fetal bovine serum (FBS), Dulbecco's modified Eagle medium (DMEM), DMEM supplemented with 2% FBS, and DMEM supplemented with 10% FBS. Few impurities were detected in the original ZnO NPs

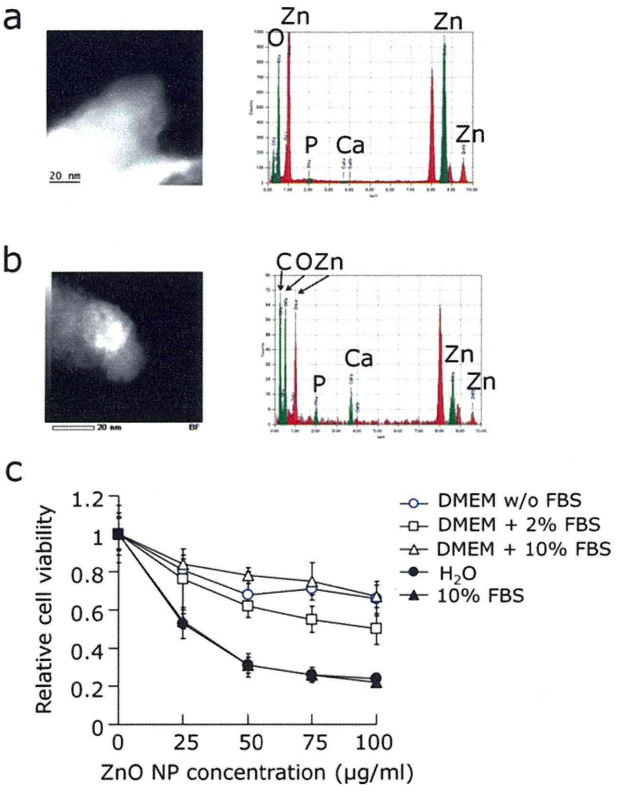

Fig. 1. Effect of dispersion medium on zinc oxide nanoparticle (ZnO NP) toxicity. (a) Purity of original ZnO NPs. Left panel: Dark-field transmission electron microscope (TEM) image of original ZnO NPs; Right panel, energy-dispersive spectroscopy (EDS) spectrum. (b) Adsorption of Ca and serum proteins on ZnO NPs dispersed in Dulbecco's modified Eagle medium (DMEM) + 10% fetal bovine serum (FBS). Left panel: Dark-field TEM image of original ZnO NPs; Right panel: EDS spectrum. (c) ZnO NPs were dispersed in H2O, 10% FBS, DMEM, DMEM + 2% FBS, or DMEM + 10% FBS. The ZnO NPs in these dispersion media were added to A549 cells cultured for 4 hr. Cell viability was assayed after 24 hr. Results are presented as the average ± S.D. $n = 4$.

(Fig. 1a), whereas calcium (Ca) was detected on the surface after dispersing ZnO NPs in DMEM supplemented with 10% FBS for 24 hr (Fig. 1b). Serum components, such as proteins, also were thought to adsorb onto the surface of ZnO NPs since carbon was detected. To examine the effect of the dispersion medium on ZnO NP toxicity, carcinoma-derived human lung epithelial A549 cells were incubated in DMEM supplemented with 10% FBS for 4 hr, and then ZnO NPs dispersed in each medium (volume, 10% of that of the culture medium) were added into the culture medium. The hydrodynamic size distribution

of ZnO NPs in culture medium was observed to be independent of the dispersion medium (Supplementary Fig. S1). Cell viability after 24-hr exposure to ZnO NPs was higher for ZnO NPs that were dispersed in DMEM and for those dispersed in DMEM supplemented with 2% and 10% FBS than for those dispersed in H_2O and 10% FBS (Fig. 1c). This suggests that the dispersion of ZnO NPs in DMEM relieves the toxicity of these NPs.

Effect of the duration of cell incubation before exposure to ZnO NPs on the toxicity of the NPs

When the cells were incubated in the culture medium without ZnO NPs, no growth was observed for 4 hr, but cell proliferation increased markedly after 24 hr and the cells achieved confluence at 72 hr (Supplementary Fig. S2a). The proportion of cells in the S-phase was higher at 24 hr and 48 hr than at 4 hr, and there were many cells in the G1-phase at 72 hr (Supplementary Fig. S2b). These observations suggest that cells are in the growth-induction stage at 4 hr, in the growth stage at 24 hr and 48 hr, and in the stationary stage at 72 hr.

When we exposed cells to ZnO NPs for various time periods, greater toxic effects were observed in 4 hr-incubated cells than in 24 hr- and 48 hr-incubated cells despite the differences in the dispersion medium (Fig. 2a, b). Thus, the toxic effect of ZnO NPs was mitigated in cells with long incubation times before exposure to ZnO NPs. Two reasons could explain the reduced toxic effect in cells incubated for a long time before exposure. One is the difference in cell density that depends on the incubation time. The 24-hr and 48-hr incubation periods resulted in higher cell density than 4-hr incubation owing to the marked increase in cell proliferation observed after 24 hr. Assuming a constant ZnO NP concentration in the culture medium, increased cell density resulted in lower numbers of ZnO NPs per cell. As such, a decrease in the number of ZnO NPs per cell may reduce the toxic effects. The second reason is the differences in physiological state arising from the cell growth stage. To examine whether toxicity depends on cell density, we seeded cells at different densities: 8,000, 16,000, and 24,000 cells/cm^2. After 4-hr incubation, the cells were exposed to ZnO NPs for 24 hr. We found that the toxicity of ZnO NPs was not dependent on cell density (Fig. 2c). Therefore, the association between incubation time and ZnO NP toxicity is likely to occur owing to the difference in the physiological state of cells, which is dependent on the growth stage of the cells.

We assessed cytotoxicity via cell viability. Cell viability was measured using a water-soluble tetrazolium/formazan (WST) assay. Cell death or impaired growth rate could reduce cell viability under cytotoxic conditions. Therefore, we investigated the main cause of the reduction in cell viability induced by ZnO NP toxicity. When ZnO NPs were added to 4 hr-, 24 hr-, and 48 hr-incubated cells at a concentration of 100 μg/mL, the proportions of dead cells were 16.1%, 17.5%, and 22%, respectively (Fig. 3). The control cells had dead cell proportions of 3.8%, 7.2%, and 7.1%, respectively (Fig. 3). As such, the percentage of dead cells attributable to ZnO NP toxicity was 12.3%, 10.3%, and 14.9% in 4 hr-, 24 hr-, and

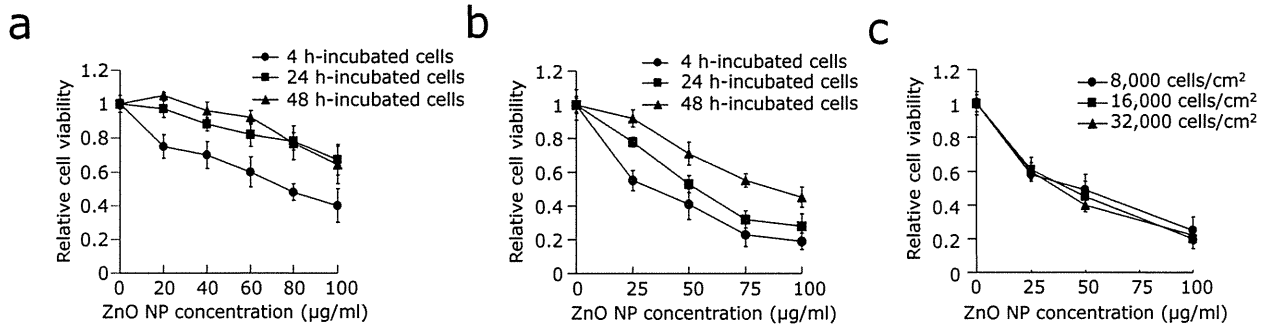

Fig. 2. Effect of the incubation time of A549 cells before exposure to zinc oxide nanoparticles (ZnO NPs) on their toxicity. (a) Toxicity of ZnO NPs dispersed in DMEM + 10% FBS. A549 cells were incubated first for 4 hr (circle), 24 hr (square), 48 hr (triangle), and then ZnO NPs dispersed in DMEM + 10% FBS were added into the medium at different concentrations. The viability of cells cultured for an additional 24 hr was assayed with the WST assay kit. Results are presented as the average ± S.D. $n = 4$. (b) Toxicity of ZnO NPs dispersed in H_2O. A549 cells were incubated first for 4 hr (circle), 24 hr (square), and 48 hr (triangle), and then ZnO NPs dispersed in H_2O were added to the medium at different concentrations. The viability of cells cultured for an additional 24 hr was assayed using the WST assay kit. Results are presented as the average ± S.D. $n = 4$. (c) Effect of cell density on the toxicity of ZnO NPs. A549 cells were cultured for 24 hr and then harvested. The harvested cells were seeded at different densities. After 4 hr of seeding, ZnO NPs in H_2O were added to the culture medium, and the cells were cultured for an additional 24 hr. Results are presented as the average ± S.D. $n = 4$.

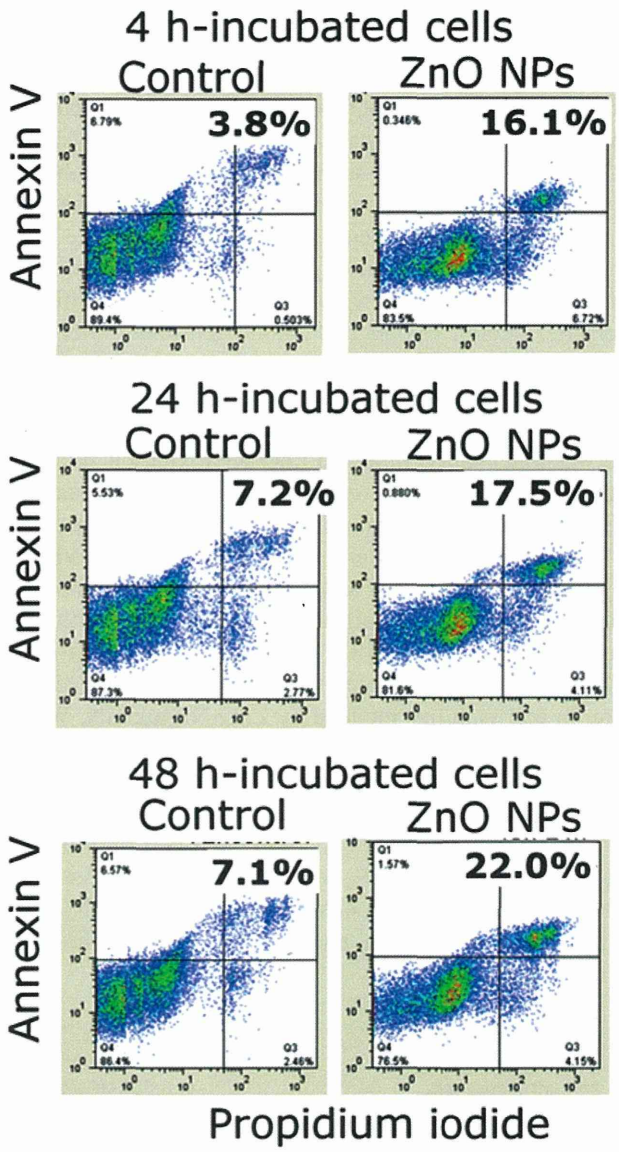

Fig. 3. Percentage of dead cells induced by the toxicity of zinc oxide nanoparticles (ZnO NPs). A549 cells were incubated for 4, 24, and 48 hr and then exposed to 100 μg/mL ZnO NPs. After culturing for an additional 24 hr, the cells were harvested and stained with propidium iodide and fluorescein isothiocyanate (FITC)-labeled annexin V. Dead cells are distributed on the right side.

48 hr-incubated cells, respectively. If cell death due to ZnO NP toxicity was caused by a reduction in cell viability, the relative cell viability might have been 87.7% (100-12.3%), 89.7% (100-10.3%), and 85.1% (100-14.9%), respectively. However, the main cause of reduction in relative cell viability by ZnO NPs was believed to be impaired growth rate rather than cell death, since the relative cell viabilities observed under these conditions were 19%, 28%, and 45%, respectively (Fig. 2b). To verify the delayed cell proliferation by ZnO NPs, we examined cell cycle distribution. Increased percentage of cells in the G1-phase were observed in the non-treated control, while a decrease in the G1-phase population was accompanied by an increase in the G2/M-phase population in cells exposed to ZnO NPs (Supplementary Fig. S3). This result suggests that the impaired growth rate by ZnO NPs is caused by G2/M arrest.

Effect of Zn ions released from ZnO NPs on the toxicity of the NPs

We examined the amount of Zn ions released from ZnO NPs in DMEM with 10% and 2% FBS. The concentration of the Zn ions released was observed to be approximately 10 μg/mL when ZnO NPs were incubated for 24 hr in the culture medium at concentrations of 75 and 100 μg/mL (Fig. 4a). FBS concentration had no effect on the amount of Zn ions released from ZnO NPs.

To test whether the Zn ions released contributed to the toxicity of ZnO NPs, we prepared culture media with zinc chloride ($ZnCl_2$) added to DMEM with 10% and 2% FBS. However, $ZnCl_2$-induced toxic effects were not observed (Fig. 4b). It is believed that Zn ions released from ZnO NPs do not contribute to the toxicity of ZnO NPs because 10 μg/mL of Zn ions is equal to approximately 20 μg/mL of $ZnCl_2$. Furthermore, we tested the toxicity of zinc phosphate [$Zn_3(PO_4)_2$] because Zn ions released from ZnO NPs may bind to the phosphate present in DMEM, which results in formation of the phosphate salt of Zn. However, $Zn_3(PO_4)_2$-induced toxicity was not observed (Fig. 4c). Therefore, the toxicity of ZnO NPs is thought to be attributed to the NPs themselves. It also has been suggested that Zn ions released from ZnO NPs form zinc-phosphate-carbonate nanosized precipitate in culture medium (Turney *et al.*, 2012), and this precipitate might protect cells from extracellular soluble zinc (Shen *et al.*, 2013).

Effect of culture medium composition on ZnO NP toxicity

We next examined the effect of FBS concentration in the culture medium (DMEM). However, no significant difference was observed in cell viability (Fig. 5a), suggesting that the FBS concentration in DMEM is not involved in the toxicity of ZnO NPs.

Next, we prepared a culture medium with DMEM diluted to 70% (70% DMEM). The 4 hr-incubated cells in 70% DMEM were exposed to ZnO NPs for 24 hr,

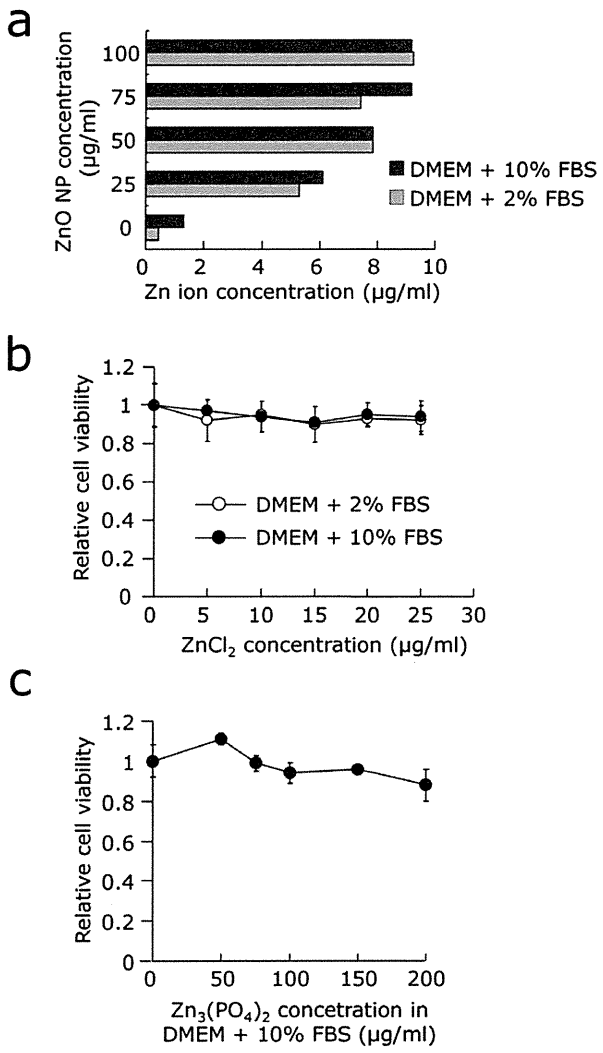

Fig. 4. Effect of Zn ions released from zinc oxide nanoparticles (ZnO NPs). (a) Level of Zn ions released from ZnO NPs. ZnO NPs were dispersed in Dulbecco's modified Eagle medium (DMEM) + 2% fetal bovine serum (FBS) and DMEM + 10% FBS at different concentrations and incubated at 37°C. After 24 hr, the concentration of Zn ions was assayed. (b) Effect of $ZnCl_2$ on the viability of A549 cells. Cells were seeded in DMEM + 10% FBS. After 4-hr incubation, the medium was replaced with DMEM + 2% FBS and DMEM + 10% FBS, each of which contained $ZnCl_2$ at different concentrations. Cell viability was assayed after an additional 24 hr culture with $ZnCl_2$. Results are presented as the average ± S.D. $n = 4$. (c) Effect of $Zn_3(PO_4)_2$ on the viability of A549 cells. The cells were incubated with DMEM + 10% FBS. After 4-hr incubation, the medium was replaced with DMEM + 10% FBS containing $Zn_3(PO_4)_2$ at different concentrations. Cell viability was assayed after an additional 24 hr culture with $Zn_3(PO_4)_2$. Results are presented as the average ± S.D. $n = 4$.

and the cell viability was compared to that obtained for DMEM without dilution. Higher levels of toxicity were seen in 70% DMEM than in DMEM without dilution (Fig. 5b). This finding suggested that some component(s) of DMEM affect(s) the toxicity of ZnO NPs. Therefore, we tested the effect of DMEM-containing salts on the toxicity. Since undiluted DMEM contains 1.8 mM calcium chloride ($CaCl_2$), 5.3 mM potassium chloride (KCl), and 0.81 mM magnesium sulfate ($MgSO_4$), the concentrations of $CaCl_2$, KCl, and $MgSO_4$ in 70% DMEM are 1.26 mM, 3.73 mM, and 0.57 mM, respectively. We added these salts to 70% DMEM to obtain elevated concentrations. The toxicity of ZnO NPs decreased as the concentration of $CaCl_2$ increased (Fig. 5c). The mitigation of ZnO NPs toxicity by Ca^{2+} was also observed in 100% DMEM without dilution (Supplementary Fig. S4). This result implies that Ca^{2+} rescues cells from the toxicity of ZnO NPs. This rescue effect was not observed for KCl and $MgCl_2$ (Fig. 5d, e). We had reported previously that CuO NPs have strong toxic effects on A549 cells (Hanagata *et al.*, 2011; Xu *et al.*, 2010). However, these cells were not rescued from the toxic effects of CuO NPs by $CaCl_2$ (Supplementary Fig. S5).

The toxicity of ZnO NPs is reported to be attributed to ROS (Hanley *et al.*, 2009; Deng *et al.*, 2009; Lin *et al.*, 2009; Xia *et al.*, 2008; Zhuang and Hanagata, 2012). In 70% DMEM containing 1.26 mM $CaCl_2$, ZnO NPs increased the number of cells that produced intracellular ROS (Fig. 6a, b). ZnO NPs also increased the number of cells that produced ROS in 70% DMEM containing 3.6 mM $CaCl_2$ (Fig. 6c, d). However, the ratio of cells that died following treatment with ZnO NPs was higher in 70% DMEM containing 1.26 mM $CaCl_2$ than in 70% DMEM containing 3.6 mM $CaCl_2$ (Fig. 6b, d). In addition, Ca^{2+} could not rescue cells from the toxicity of extracellular oxidative stress (Fig. 5f). These results suggest that Ca^{2+} is not involved in quenching ROS, although Ca^{2+} rescued cells from the toxicity of ZnO NPs.

Change in the cellular response due to Ca^{2+} inferred from global gene expression analysis

To examine the mechanism by which Ca^{2+} rescues cells from the toxicity of ZnO NPs, genes with alterations in expression levels were identified using DNA microarray analysis. These gene expression data have been deposited in the Gene Expression Omnibus database with the accession code GSE43003. We identified one upregulated gene and seven downregulated genes in cells cultured in 70% DMEM containing 3.6 mM $CaCl_2$, as compared to the gene expression observed in cells cultured in 70% DMEM containing 1.26 mM $CaCl_2$ (Table 1). However,

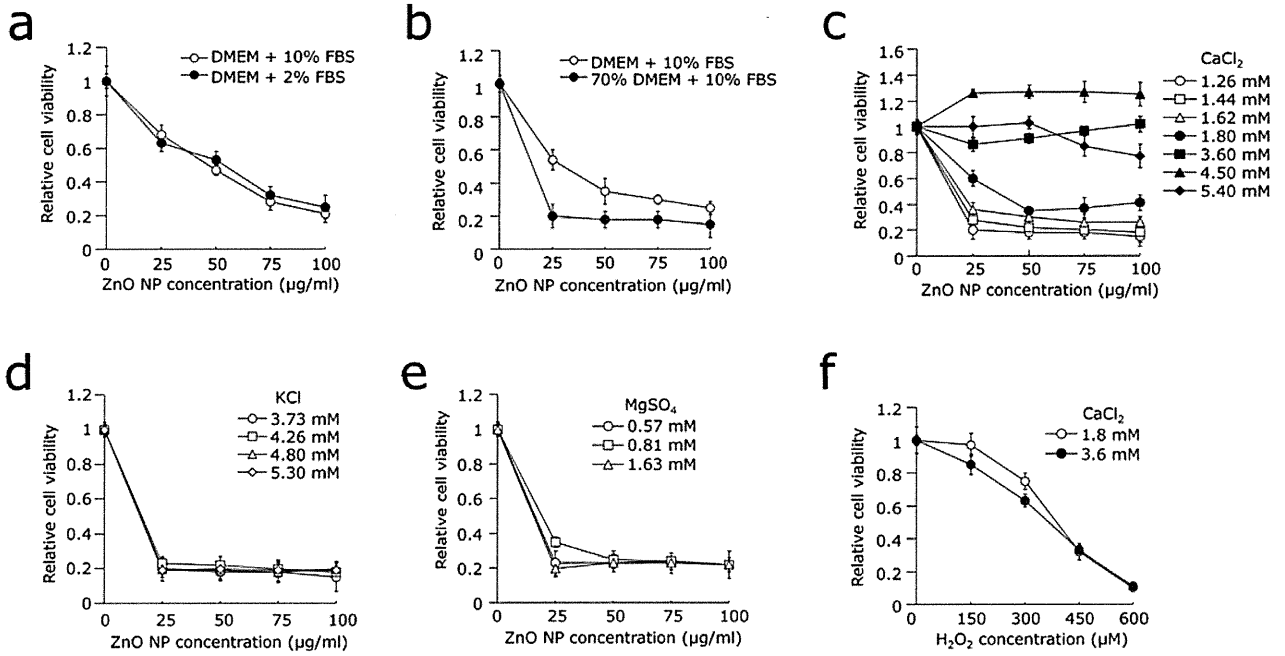

Fig. 5. Effect of medium components on the toxicity of zinc oxide nanoparticles (ZnO NPs). (a) Effect of fetal bovine serum (FBS) concentration. The cells were incubated with Dulbecco's modified Eagle medium (DMEM) + 10% FBS for 4 hr, and the medium then was replaced with DMEM + 10% FBS and DMEM + 2% FBS, each of which contained ZnO NPs at different concentrations. Cell viability was assayed after culturing for an additional 24 hr with ZnO NPs. Results are presented as the average ± S.D. $n = 4$. (b) Effect of dilution of the medium. The cells were incubated with DMEM + 10% FBS for 4 hr, and the medium then was replaced with DMEM + 2% FBS and DMEM + 10% FBS, each of which contained ZnO NPs at different concentrations. Cell viability was assayed after culturing for an additional 24 hr with ZnO NPs. Results are presented as the average ± S.D. $n = 4$. (c,d,e) Effect of metal salts on viability of cells exposed to ZnO NPs. The cells were incubated with DMEM + 10% FBS for 4 hr, and the medium then was replaced with ZnO NPs containing 70% DMEM + 10% FBS with different concentrations of $CaCl_2$, KCl, or $MgSO_4$. Cell viability was assayed after culturing for an additional 24 hr with ZnO NPs. Results are presented as the average ± S.D. $n = 4$. (c) $CaCl_2$. The 70% DMEM contained 1.26 mM $CaCl_2$. (d) KCl. The 70% DMEM contained 3.73 mM KCl. (e) $MgSO_4$. The 70% DMEM used contained 0.57 mM $MgSO_4$. (f) Effect of $CaCl_2$ concentration on oxidative stress-induced toxicity. The cells were incubated with DMEM + 10% FBS for 4 hr, and the medium then was replaced with 70% DMEM + 10% FBS containing $CaCl_2$ at concentrations of 1.26 mM and 3.6 mM. The cells were exposed to H_2O_2 immediately after replacing the medium. Cell viability was assayed after culturing for an additional 24 hr with H_2O_2. Results are presented as the average ± S.D. $n = 4$.

Table 1. The number of changed genes in cells cultured in medium containing 3.6 mM $CaCl_2$ when compared with gene expression in cells cultured in medium containing 1.26 mM $CaCl_2$.

	ZnO NPs		
	0 μg/mL	25 μg/mL	100 μg/mL
Number of valid genes[a)]	13,708	12,869	12,085
Number of upregulated genes[b)]	1	886	1,055
Number of downregulated genes[c)]	7	1,155	1,151

[a)] Total 19,595 genes were analyzed by DNA microarray. The valid genes were reproducible genes whose expression level was within 2-fold in two analyses.

[b)] The number of genes whose expression level was more than 2-fold in cells cultured in 70% diluted Dulbecco's modified Eagle medium (DMEM) containing 3.6 mM $CaCl_2$ when compared with that in cells cultured in 70% DMEM containing 1.26 mM $CaCl_2$.

[c)] The number of genes whose expression level was less than 2-fold in cells cultured in 70% DMEM containing 3.6 mM $CaCl_2$ when compared with that in cells cultured in 70% DMEM containing 1.26 mM $CaCl_2$.

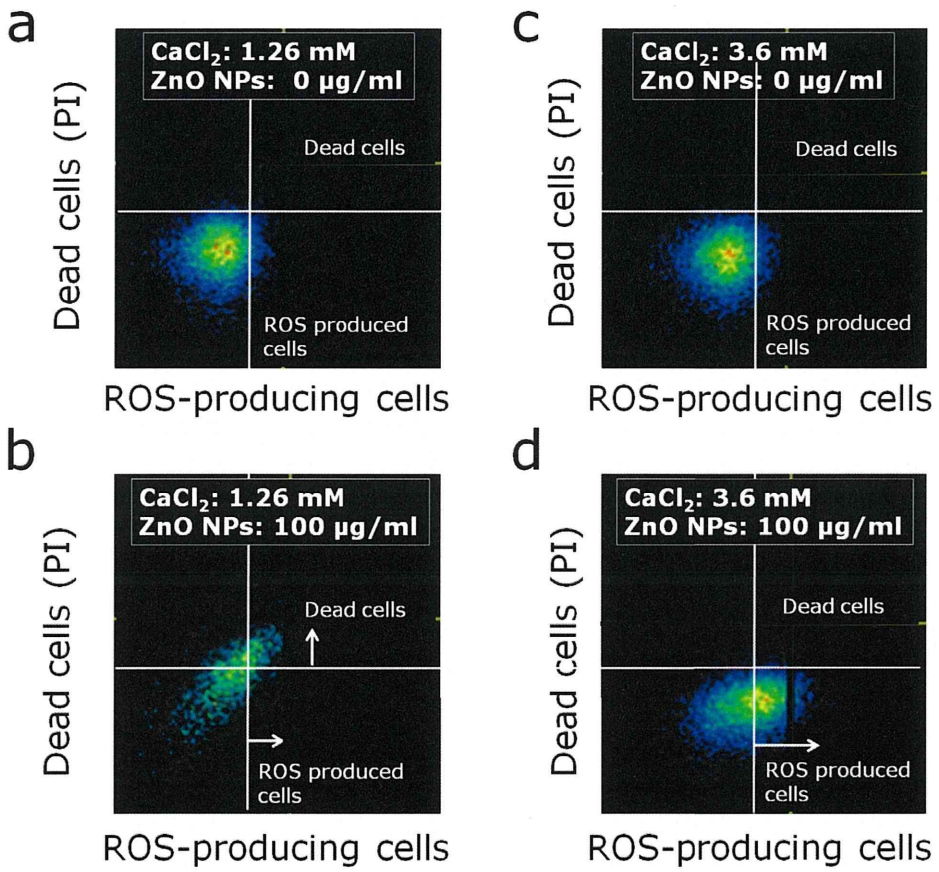

Fig. 6. Effect of $CaCl_2$ concentration on reactive oxygen species (ROS) quenching. The cells were incubated with Dulbecco's modified Eagle medium (DMEM) + 10% fetal bovine serum (FBS) for 4 hr, and the medium then was replaced with 70% DMEM + 10% FBS containing $CaCl_2$ at concentrations of 1.26 mM (a, b) and 3.6 mM (c, d). The cells were exposed to 0 μg/mL (a, c) and 100 μg/mL (b, d) ZnO NPs immediately following replacing the medium. Intracellular ROS and dead cells were analyzed with fluorescence-activated cell sorting (FACS) 24 hr after the addition of ZnO NPs.

no statistically significant functional category was generated by these genes with altered expression, as determined using Gene Ontology (GO) analysis. This finding suggests that the increase in Ca^{2+} concentration of the culture medium without ZnO NPs has no effect on the function of normal cells.

In the presence of 25 μg/mL ZnO NPs, 886 upregulated genes and 1155 downregulated genes were identified in cells cultured in 70% DMEM containing 3.6 mM $CaCl_2$, as compared to the gene expression observed in cells cultured in 70% DMEM containing 1.26 mM $CaCl_2$ (Table 1). We also identified 1055 upregulated and 1151 downregulated genes in the presence of 100 μg/mL ZnO NPs (Table 1). GO analysis generated functional categories that were significantly altered owing to upregulation of gene expression induced by the increase in Ca^{2+} concentration (Table 2). All the categories were involved in the cell cycle. These results imply that Ca^{2+} promotes cell division in cells exposed to ZnO NPs; Ca^{2+} had no effect on unexposed cells. GO analysis using downregulated genes generated significant functional categories involved in the metabolic process (Supplementary Table S1).

DISCUSSION

The toxicity of ZnO NPs has been the subject of many studies. However, the levels of this toxicity vary widely, with major toxicity being demonstrated in some studies and hardly any toxicity in others. Different cell types have different levels of sensitivity to the toxicity of ZnO NPs (Hanley *et al.*, 2009; Ostrovsky *et al.*, 2009). However, there has been little discussion of whether other fac-

Table 2. Top ten significantly changed Gene Ontology (GO) categories of upregulated genes in cells cultured in medium containing 3.6 mM $CaCl_2$.

ZnO NPs =25 μg/mL			ZnO NPs =100 μg/mL		
GO ID	GO term	p-value	GO ID	GO term	p-value
GO:0000087	M phase of mitotic cell cycle	8.52E-44	GO:0022403	Cell cycle phase	5.10E-89
GO:0000280	Nuclear division	1.48E-43	GO:0000278	Mitotic cell cycle	2.23E-79
GO:0007067	Mitosis	1.48E-43	GO:0000279	M phase	3.81E-68
GO:0022403	Cell cycle phase	1.55E-43	GO:0000087	M phase of mitotic cell cycle	2.71E-64
GO:0000278	Mitotic cell cycle	6.83E-43	GO:0000280	Nuclear division	3.24E-64
GO:0000279	M phase	3.26E-42	GO:0007067	Mitosis	3.24E-64
GO:0022402	Cell cycle process	7.95E-42	GO:0048285	Organelle fission	4.32E-62
GO:0048285	Organelle fission	2.41E-41	GO:0006259	DNA metabolic process	2.56E-51
GO:0007049	Cell cycle	2.43E-41	GO:0051301	Cell division	2.65E-50
GO:0051301	Cell division	2.11E-32	GO:0006260	DNA replication	5.72E-40

tors, such as culture conditions, could have any effect on the cytotoxicity of ZnO NPs. In this study, we have shown that even cells of the same type can have differing sensitivity to ZnO NP toxicity, depending on differences in the dispersion medium, physiological states arising from the cell growth stage, and the composition of the culture medium. Moreover, we also suggest that the toxicity of ZnO NPs is not influenced largely by extracellular Zn ions released from these particles. It has been suggested that ZnO NPs taken up into endolysosome generate ROS, which leads to apoptosis owing to the increase in caspase-3 and caspase-7 activity (Syama *et al.*, 2014). We previously observed intracellular ROS production in A549 cells exposed to ZnO NPs (Zhuang *et al.*, 2012), but this study revealed that ZnO NPs cause toxicity via the retardation of cell growth rate by G2-phase arrest rather than from the induction of apoptosis. It also has been reported by Goncalves and Girard (2014) and Lu *et al.* (2015) that the induction of apoptosis is not a major cause of ZnO NPs toxicity.

The toxicity of ZnO NPs on A549 cells is highly dependent on the concentration of Ca^{2+} in the culture medium. When DMEM is diluted to 70%, it seems that the lower concentration of Ca^{2+} in the culture medium makes the cells more sensitive to ZnO NP toxicity causing them to sustain greater damage. We found that a dispersion of ZnO NPs in H_2O has greater toxicity effects than a dispersion of ZnO NPs in DMEM. This difference is thought to originate from the dilution of the DMEM culture medium in which the cells were being cultivated by the addition of the aqueous dispersion.

Increased concentrations of Ca^{2+} in the culture medium mitigate the cell damage caused by the toxicity of ZnO NPs. In the absence of ZnO NPs, GO analysis based on changes in gene expression showed no large difference in the physiological state of cells cultured in 70% DMEM containing 1.26 mM $CaCl_2$ or in 70% DMEM containing 3.6 mM $CaCl_2$. However, in the presence of ZnO NPs, an increase in the Ca^{2+} concentration caused marked improvement in the expression of gene groups that contribute to the cell cycle. Since the expression of these gene groups is not enhanced in the absence of ZnO NPs, it seems that the enhanced expression of gene groups that contribute to the cell cycle is a defense mechanism of the cells against ZnO NP toxicity. The toxicity had a greater effect retardation of cell growth than on induction of cell death. Thus, it seems that the effect of Ca^{2+} on enhancing the expression of gene groups associated with the cell cycle is that of reversing the retarded cell growth. Ca^{2+} was also detected on the surface of ZnO NPs dispersed in DMEM. The lower toxicity of ZnO NPs dispersed in DMEM compared with that of ZnO NPs dispersed in H_2O may be because of simultaneous uptake of ZnO NPs and Ca^{2+} by the cells.

The toxicity of ZnO NPs has been reported to originate from the generation of ROS (Hanley *et al.*, 2009; Deng *et al.*, 2009; Lin *et al.*, 2009; Xia *et al.*, 2008; Zhuang and Hanagata, 2012). Furthermore, it has been suggested that the toxicity of silicon dioxide (SiO_2) NPs against RAW264.7 cells is owing to the increase in the intracellular concentration of Ca^{2+} as well as from the generation of ROS (Yang *et al.*, 2009). This increase in the intracellular Ca^{2+} concentration also has been observed in human bronchial epithelial cells (BEAS-2B) exposed to ZnO NPs (Huang *et al.*, 2010) and in cells exposed to Ag NPs (Moutin *et al.*, 1989; AshaRani *et al.*, 2009a, 2009b).

The toxicity of ZnO NPs against BEAS-2B cells decreases after treatment with the antioxidant *N*-acetylcysteine (NAC), but since NAC also blocks the influx of Ca^{2+} ions into the cell, it appears that the increase in ROS generation and intracellular Ca^{2+} concentration jointly contribute to toxicity (Huang *et al.*, 2010). However, in this study, the cytotoxicity of ZnO NPs was mitigated by increasing the Ca^{2+} concentration in the culture medium. This result seems to suggest that the increase in the intracellular concentration of Ca^{2+} ions in conjunction with the increase in ROS does not contribute to toxicity but rather is a defense mechanism to counteract the toxicity.

Taken together, this study revealed that the sensitivity of human lung epithelial cells to ZnO NPs differed depending on the dispersing medium, the physiological state of the cells resulting from their growth stage, and the composition of the medium. The study also revealed that Zn ions released from ZnO NPs did not contribute greatly to the cytotoxicity of ZnO NPs. ZnO NPs affected cells by slowing down the rate of cell proliferation but not by inducing cell death. When the concentration of Ca^{2+} in the medium increased, the cytotoxicity of ZnO NPs was mitigated. This result suggests that the expression of cell cycle-related genes increased due to Ca^{2+} and that the cycle proliferation rate recovered.

ACKNOWLEDGEMENTS

This work was supported by a Grant-in-Aid from the Ministry of Health, Labour, and Welfare of Japan.

Conflict of interest---- The authors declare that there is no conflict of interest.

REFERENCES

Agren, M.S. and Mirastschijski, U. (2004): The release of zinc ions from and cytocompatibility of two zinc oxide dressings. J. Wound. Care, **13**, 367-369.

Ai, H., Bu, Y. and Han, K. (2003): Glycine-Zn^{+}/Zn^{2+} and their hydrates: on the number of water molecules necessary to stabilize the zwitterionic glycine-Zn^{+}/Zn^{2+} over the nonzwitterionic ones. J. Chem. Phys., **118**, 10973-10985.

AshaRani, P.V., Hande, M.P. and Valiyaveettil, S. (2009a): Anti-proliferative activity of silver nanoparticles. BMC Cell Biol., **10**, 65.

AshaRani, P.V., Low Kah, M.G., Hande, M.P. and Valiyaveettil, S. (2009b): Cytotoxicity and genotoxicity of silver nanoparticles in human cells. ACS Nano, **3**, 279-290.

Brown, J.J. (1988): Zinc fume fever. Br. J. Radiol., **61**, 327-329.

Brown, D.M., Wilson, M.R., MacNee, W., Stone, V. and Donaldson, K. (2001): Size-dependent proinflammatory effects of ultrafine polystyrene particles: a role for surface area and oxidative stress in the enhanced activity of ultrafines. Toxicol. Appl. Pharmacol., **175**, 191-199.

Conner, M.W., Flood, W.H., Rogers, A.E. and Amdur, M.O. (1998): Lung injury in guinea pigs caused by multiple exposures to ultrafine zinc oxide: changes in pulmonary lavage fluid. J. Toxicol. Environ. Health, **25**, 57-69.

Deng, X., Luan, Q., Chen, W., Wang, Y., Wu, M., Zhang, H. and Jiao, Z. (2009): Nanosized zinc oxide particles induce neural stem cell apoptosis. Nanotechnology, **20**, 115101.

Donaldson, K. and Tran, C.L. (2002): Inflammation caused by particles and fibers. Inhal. Toxicol., **14**, 5-27.

Fine, J.M., Gordon, T., Chen, L.C., Kinney, P., Falcone, G. and Beckett, W.S. (1997): Metal fume fever: characterization of clinical and plasma IL-6 responses in controlled human exposures to zinc oxide fume at and below the threshold limit value. J. Occup. Environ. Med., **39**, 722-726.

Franklin, N.M., Rogers, N.J., Apte, S.C., Batley, G.E., Gadd, G.E. and Casey, P.S. (2007): Comparative toxicity of nanoparticulate ZnO, bulk ZnO, and $ZnCl_2$ to a freshwater microalga (Pseudokirchneriella subcapitata): the importance of particle solubility. Environ. Sci. Technol., **41**, 8484-8490.

Goncalves, D.M. and Girard, D. (2014): Zinc oxide nanoparticles delay human neutrophil apoptosis by a de novo protein synthesis-dependent and reactive oxygen species-independent mechanism. Toxicol. In Vitro, **28**, 926-931.

Hanagata, N., Xu, M., Takemura, T. and Zhuang, F. (2010): Cellular response to ZnO nanoparticle toxicity inferred from global gene expression profiles. Nano Biomed., **2**, 153-169.

Hanagata, N., Zhuang, F., Connolly, S., Li, J., Ogawa, N. and Xu, M. (2011): Molecular responses of human lung epithelial cells to the toxicity of copper oxide nanoparticles inferred from whole genome expression analysis. ACS Nano, **5**, 9326-9338.

Hanley, C., Thurber, A., Hanna, C., Punnoose, A., Zhang, J. and Wingett, D.G. (2009): The influences of cell type and ZnO nanoparticle size on immune cell cytotoxicity and cytokine induction. Nanoscale Res. Lett., **4**, 1409-1420.

Huang, C.C., Aronstam, R.S., Chen, D.-R. and Huang, Y.-W. (2010): Oxidative stress, calcium homeostasis, and altered gene expression in human lung epithelial cells exposed to ZnO nanoparticles. Toxicol. In Vitro, **24**, 45-55.

Huang, Z., Zheng, X., Yan, D., Yin, G., Liao, X., Kang, Y., Yao, Y., Huang, D. and Hao, B. (2008): Toxicological effect of ZnO nanoparticles based on bacteria. Langmuir, **24**, 4140-4144.

Ji, S. and Ye, C. (2008): Synthesis, growth mechanism, and applications of zinc oxide nanomaterials. J. Mater. Sci. Technol., **24**, 457-472.

Krezel, A., Hao, Q. and Maret, W. (2007): The zinc/thiolate redox biochemistry of metallothionein and the control of zinc ion fluctuations in cell signaling. Arch. Biochem. Biophys., **463**, 188-200.

Kuschner, W.G., D'Alessandro, A., Wintermeyer, S.F., Wong, H., Boushey, H.A. and Blanc, P.D. (1995): Pulmonary responses to purified zinc oxide fume. J. Investig. Med., **43**, 371-378.

Lam, H.F., Chen, L.C., Ainsworth, D., Peoples, S. and Amdur, M.O. (1988): Pulmonary function of guinea pigs exposed to freshly generated ultrafine zinc oxide with and without spike concentrations. Am. Ind. Hyg. Assoc. J., **49**, 333-341.

Lin, W., Xu, Y., Huang, C.-C., Ma, Y., Shannon, K.B., Chen, D.-R. and Huang, Y.-W. (2009): Toxicity of nano- and micro-sized ZnO particles in human lung epithelial cells. J. Nanopart. Res., **11**, 25-39.

Liu, Y., He, L., Mustapha, A., Li, H., Hu, Z.Q. and Lin, M. (2009): Antibacterial activities of zinc oxide nanoparticles against

Escherichia coli O157:H7. J. Appl. Microbiol., **107**, 1193-1201.

Lu, S., Zhang, W., Zhang, R., Liu, P., Wang, Q., Shang, Y., Wu, M., Donaldson, K. and Wang, Q. (2015): Comparison of cellular toxicity caused by ambient ultrafine particles and engineered metal oxide nanoparticles. Part. Fibre Toxicol., **12**, 5.

Moos, P.J., Chung, K., Woessner, D., Honeggar, M., Cutler, N.S. and Veranth, J.M. (2010): ZnO particulate matter requires cell contact for toxicity in human colon cancer cells. Chem. Res. Toxicol., **23**, 733-739.

Moutin, M.J., Abramson, J.J., Salama, G. and Dupont, Y. (1989): Rapid Ag^{+}-induced release of Ca^{2+} from sarcoplasmic reticulum vesicles of skeletal muscle: a rapid filtration study. Biochem. Biophys., Acta, **984**, 289-292.

Newman, M.D., Stotland, M. and Ellis, J.I. (2009) The safety of nanosized particles in titanium dioxide- and zinc oxide-based sunscreens. J. Am. Acad. Dermatol., **61**, 685-692.

Osmond, M.J. and McCall, M.J. (2010): Zinc oxide nanoparticles in modern sunscreens: an analysis of potential exposure and hazard. Nanotoxicology, **4**, 15-41.

Ostrovsky, S., Kazimirsky, G., Gedanken, A. and Brodie, C. (2009): Selective cytotoxic effect of ZnO nanoparticles on glioma cells. Nano Res., **2**, 882-890.

Overbeck, S., Uciechowski, P., Ackland, M.L., Ford, D. and Rink, L. (2008): Intracellular zinc homeostasis in leukocyte subsets is regulated by different expression of zinc exporters ZnT-1 to ZnT-9. J. Leukoc. Biol., **83**, 368-380.

Prasad, A.S. (2008): Zinc in human health: effect of zinc on immune cells. Mol. Med., **14**, 353-357.

Reddy, K.M., Feris, K., Bell, J., Wingett, D.G., Hanley, C. and Punnoose, A. (2007): Selective toxicity of zinc oxide nanoparticles to prokaryotic and eukaryotic systems. Appl. Phys. Lett., **90**, 213902-1-213902-3.

Shen, C., James, S.A., de Jonge, M.D., Turney, T.W., Wright, P.F. A. and Feltis, B.N. (2013): Relating cytotoxicity, zinc ions, and reactive oxygen in ZnO nanoparticle-exposed human immune cells. Toxicol. Sci., **136**, 120-130.

Song, W., Zhang, J., Gao, J., Zhang, J., Ding, F., Li, L. and Sun, Z. (2010): Role of the dissolved zinc ion and reactive oxygen species in cytotoxicity of ZnO nanoparticles. Toxicol. Lett., **199**, 389-397.

Stefanidou, M., Maravelias, C., Dona, A. and Spiliopoulou, C. (2006): Zinc: a multipurpose trace element. Arch. Toxicol., **80**, 1-9.

Syama, S., Sreekanth, P.J., Varma, H.K. and Mohanan, P.V. (2014): Zinc oxide nanoparticles induced oxidative stress in mouse bone marrow mesenchymal stem cells. Toxicol. Mech. Methods, **24**, 644-653.

Turney, T.W., Duriska, M.B., Jayaratne, V.N., Elbaz, A., O'Keefe, S.J., Hastings, A.S., Piva, T.J., Wright, P.F. and Feltis, B.N. (2012) Formation of zinc-containing nanoparticles from Zn^{2+} ions in cell culture media: Implications for the nanotoxicology of ZnO. Chem. Res. Toxicol., **25**, 2057-2066.

Vallee, B.L. and Falchuk, K.H. (1993): The biochemical basis of zinc physiology. Physiol. Rev., **73**, 79-118.

Vandebriel, R.J. and De Jong, W.H. (2012): A review of mammalian toxicity of ZnO nanoparticles. Nanotechnol. Sci. Appl., **5**, 61-71.

Vogelmeier, C., König, G., Bencze, K. and Fruhmann, G. (1987) Pulmonary involvement in zinc fume fever. Chest, **92**, 946-948.

Warheit, D.B., Sayes, C.M. and Reed, K.L. (2009): Nanoscale and fine zinc oxide particles: can *in vitro* assays accurately forecast lung hazards following inhalation exposures? Environ. Sci. Technol., **43**, 7939-7945.

Xia, T., Kovochich, M., Liong, M., Mädler, L., Gilbert, B., Shi, H., Yeh, J.I., Zink, J.I. and Nel, A.E. (2008): Comparison of the mechanism of toxicity of zinc oxide and cerium oxide nanoparticles based on dissolution and oxidative stress properties. ACS Nano, **2**, 2121-2134.

Xu, M., Fujita, D., Kajiwara, S., Minowa, T., Li, X., Takemura, T., Iwai, H. and Hanagata, N. (2010): Contribution of physicochemical characteristics of nano-oxides to cytotoxicity. Biomaterials, **31**, 8022-8031.

Xu, L., Takemura, T., Xu, M. and Hanagata, N. (2011): Toxicity of siliver nanoparticles as assessed by global gene expression analysis. Mater. Express, **1**, 74-79.

Yang, S.T., Liu, J.H., Wang, J. Yuan, Y., Cao, A., Wang, H., Liu, Y. and Zhao, Y. (2010): Cytotoxicity of zinc oxide nanoparticles: importance of microenvironment. J. Nanosci. Nanotechnol., **10**, 8638-8645.

Yang, H., Wu, Q., Tang, M., Kong, L. and Lu, Z. (2009): Cell membrane injury induced by silica nanoparticles in mouse macrophage. J. Biomed. Nanotech., **5**, 528-535.

Zhang, L., Jiang, Y., Ding, Y., Daskalakis, N., Jeuken, L., Povey, M., O'Neill, A.J. and York, D.W. (2010) Mechanistic investigation into antibacterial behavior of suspensions of ZnO nanoparticles against E.coli. J. Nanopart. Res., **12**, 1625-1636.

Zhang, Y., Nguyen, K.C., Lefebvre, D.E., Shwed, P.S., Crosthwait, J., Bondy, G.S. and Tayabali, A.F. (2014): Critical experimental parameters related to the cytotoxicity of zinc oxide nanoparticles. J. Nanopart. Res., **16**, 2440.

Zhuang, F. and Hanagata, N. (2012): Synergic toxicity of solid particles and released zinc from zinc oxide nanoparticles to human lung epithelial cells. Nano Biomed., **4**, 90-112.

International Journal of Nanomedicine

Dovepress

open access to scientific and medical research

Open Access Full Text Article

ORIGINAL RESEARCH

Silver nanoparticles induce tight junction disruption and astrocyte neurotoxicity in a rat blood–brain barrier primary triple coculture model

Liming Xu[1,2,*]
Mo Dan[1,*]
Anliang Shao[1]
Xiang Cheng[1,3]
Cuiping Zhang[4]
Robert A Yokel[5]
Taro Takemura[6]
Nobutaka Hanagata[6]
Masami Niwa[7,8]
Daisuke Watanabe[7,8]

[1]National Institutes for Food and Drug Control, No 2, Temple of Heaven, Beijing, [2]School of Information and Engineering, Wenzhou Medical University, Wenzhou, [3]School of Materials Science and Engineering, Southwest Jiaotong University, Chengdu, [4]Beijing Neurosurgical Institute, Capital Medical University, Beijing, People's Republic of China; [5]College of Pharmacy, University of Kentucky, Lexington, KY, USA; [6]Nanotechnology Innovation Station for Nanoscale Science and Technology, National Institute for Materials Science, Tsukuba, Ibaraki, [7]Department of Pharmacology, Nagasaki University, [8]BBB Laboratory, PharmaCo-Cell Company, Ltd., Nagasaki, Japan

*These authors contributed equally to this work

Correspondence: Liming Xu; Mo Dan
National Institutes for Food and Drug Control, No 2, Temple of Heaven, Beijing 100050, People's Republic of China
Tel/fax +86 10 6709 5661;
+86 10 6787 2233 ext 8220
Email xuliming@nifdc.org.cn;
danmo@nifdc.org.cn

Background: Silver nanoparticles (Ag-NPs) can enter the brain and induce neurotoxicity. However, the toxicity of Ag-NPs on the blood–brain barrier (BBB) and the underlying mechanism(s) of action on the BBB and the brain are not well understood.

Method: To investigate Ag-NP suspension (Ag-NPS)-induced toxicity, a triple coculture BBB model of rat brain microvascular endothelial cells, pericytes, and astrocytes was established. The BBB permeability and tight junction protein expression in response to Ag-NPS, NP-released Ag ions, and polystyrene-NP exposure were investigated. Ultrastructural changes of the microvascular endothelial cells, pericytes, and astrocytes were observed using transmission electron microscopy (TEM). Global gene expression of astrocytes was measured using a DNA microarray.

Results: A triple coculture BBB model of primary rat brain microvascular endothelial cells, pericytes, and astrocytes was established, with the transendothelial electrical resistance values >200 $\Omega \cdot cm^2$. After Ag-NPS exposure for 24 hours, the BBB permeability was significantly increased and expression of the tight junction (TJ) protein ZO-1 was decreased. Discontinuous TJs were also observed between microvascular endothelial cells. After Ag-NPS exposure, severe mitochondrial shrinkage, vacuolations, endoplasmic reticulum expansion, and Ag-NPs were observed in astrocytes by TEM. Global gene expression analysis showed that three genes were upregulated and 20 genes were downregulated in astrocytes treated with Ag-NPS. Gene ontology (GO) and Kyoto Encyclopedia of Genes and Genomes (KEGG) pathway analysis showed that the 23 genes were associated with metabolic processes, biosynthetic processes, response to stimuli, cell death, the MAPK pathway, and so on. No GO term and KEGG pathways were changed in the released-ion or polystyrene-NP groups. Ag-NPS inhibited the antioxidant defense of the astrocytes by increasing thioredoxin interacting protein, which inhibits the Trx system, and decreasing *Nr4a1* and *Dusp1*. Meanwhile, Ag-NPS induced inflammation and apoptosis through modulation of the MAPK pathway or B-cell lymphoma-2 expression or mTOR activity in astrocytes.

Conclusion: These results draw our attention to the importance of Ag-NP-induced toxicity on the neurovascular unit and provide a better understanding of its toxicological mechanisms on astrocytes.

Keywords: Ag nanoparticles, astrocytes, BBB model, global gene expression analysis, antioxidant defense

Introduction

Silver nanoparticles (Ag-NPs) are 1 to 100 nm-sized metallic colloidal particles widely used in engineering, manufacturing, and biomedicine. Compared to bulk silver metal, Ag-NPs showed greater efficacy against bacteria due to their relatively large

submit your manuscript | www.dovepress.com
Dovepress
http://dx.doi.org/10.2147/IJN.S85265